

D. Characterization of New Amberlyst Catalysts

Three new Amberlyst solid acid resin catalysts, designated as Amberlyst-35, -36, and -1010, were obtained from Rohm and Haas. These newer Amberlyst catalysts have polymeric structures similar to that of the Amberlyst-15 resin that was extensively studied earlier in this project, e.g. see Figure 5. The main differences in these new catalysts compared to Amberlyst-15 are that the Amberlyst-35 and -36 resins are more thermally stable and have higher acidity, while the Amberlyst-1010 resin has a much higher surface area, smaller average pore size, and lower concentration of acid sites. The new catalysts were characterized by means of surface area, swelling properties, and concentration of acid sites.

Surface Area Measurements

Surface areas were measured using a Micromeritics Gemini 2360 Surface Area Analyzer with nitrogen gas as the adsorbate at -196°C . The Amberlyst catalysts were dried at 90°C overnight under nitrogen atmosphere prior to the surface area measurements. Results were obtained as BET multipoint and Langmuir surface areas. Data points were chosen so that p/p_0 varied from 0.05 to 0.3. This yielded a linear BET plot.

Table 7 shows the results for the three Amberlyst samples. It can be seen that the Langmuir surface area results corresponded well with the values given by the manufacturer. The reason for the apparent low values determined by the BET method is not yet known. It was not specified by the manufacturer what type of surface area model was used or what adsorbate was used. The surface area of the Amberlyst-15 resin used for comparison was approximately $45 \text{ m}^2/\text{g}$.

Figure 5. Schematic of Amberlyst structure.

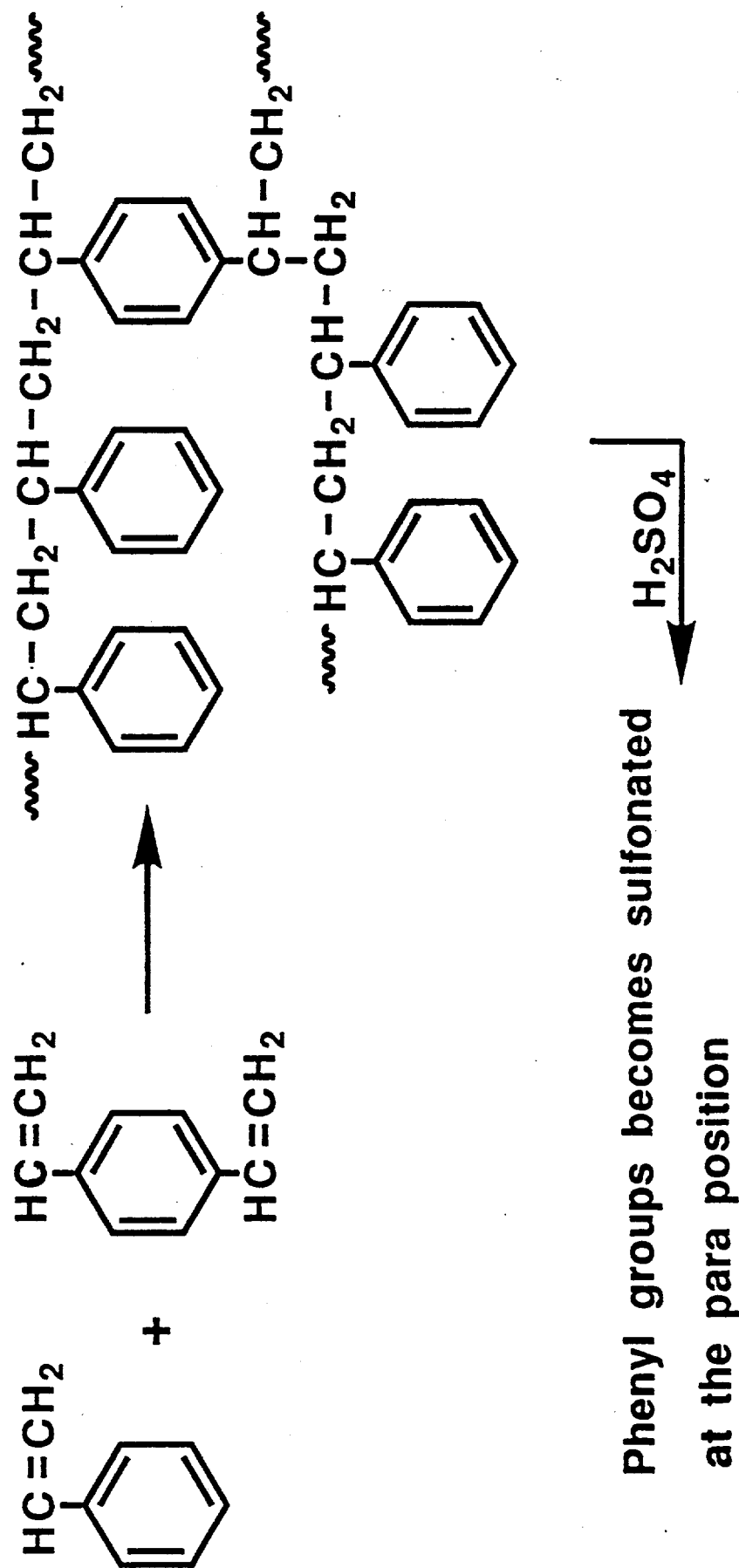


Table 7. Surface Areas of the Amberlyst Resins

Amberlyst	Manufacturer's Surface Area (m ² /g)	Experimental BET Multipoint Surface Area (m ² /g)	Experimental Langmuir Surface Area (m ² /g)
1010	540	350	570
35	44	32	50
36	35	19	31

Swelling Properties of the Resins

To measure the swelling properties of the Amberlyst samples, approximately 1.5 g of each catalyst was mixed with 4.0 ml of solvent in a graduated cylinder. The percent swelling was measured in both methanol and water. The dry volume of the resin was taken immediately following the addition of the catalyst to the solvent. After an equilibration time of 5-10 minutes, the volume of the resin was recorded once again. This final volume was the volume after swelling. The % swelling was then calculated by taking the difference of the two volumes.

Amberlyst-35 and -36 were obtained from the manufacturer in a wet form, and they were dried overnight at 90°C to remove water before the swelling experiments were carried out. Amberlyst-1010, according to the manufacturer's data, contained less than 2% water and was not dried further. Table 8 shows the results obtained from the swelling experiments. All three catalysts swelled more in water than in methanol. Amberlyst-35 and -36 were very similar in their swelling properties, but Amberlyst-1010 swelled significantly less. One possible reason for the smaller swelling of Amberlyst-1010 is that this resin has appreciably smaller average diameter of its internal pores ($\approx 50\text{\AA}$) than the Amberlyst-35 and -36 resins. This indicates more cross-linking and a more rigid polymer network.

Table 8. % Swelling of Amberlyst Resins in Water and Methanol

Amberlyst	% Swelling in water	% Swelling in methanol
1010	25	22
35	58	50
36	52	42

Concentration of Acid Sites in the Resins

The ion exchange capacities provided by the manufacturer were verified by titration of the Amberlyst samples in water with 0.498 M sodium hydroxide. Amberlyst-35 and -36 resins were dried at 90°C in air overnight prior to weighing and titration, while the Amberlyst-1010 was used as received. The pH was continuously monitored throughout the titration with a pH meter, which providing an acid-base titration curve, where the inflection point gave the end point of the titration.

Table 9 includes both the manufacturer's value of the ion exchange capacities and the experimental ion exchangeable H⁺ concentrations in meq/g of the dry resin, as well as the % difference involved in the experimental results. It is seen that the experimental values obtained in this laboratory agree very well with the manufacturer's specifications. Again, the Amberlyst-35 and -36 resins had very similar properties, whereas the Amberlyst-1010 had a much lower concentration of acid sites.

Table 9. Ion Exchange Titration Data for Amberlyst-1010, -35, and -36 Resins.

Amberlyst	Manufacturer's meq/g	LU Experimental meq/g	% Difference
1010	3.3	3.25	1.5
35	5.2	5.22	0.4
36	5.4	5.30	1.8

Catalytic Activities and Selectivities of the Amberlyst Catalysts

The new Amberlyst-35 and -36 catalysts were reported to be more acidic than Amberlyst-15, and the Amberlyst-1010 resin has a higher porosity ($0.41 \text{ cm}^3/\text{g}$) than the other three resins. Higher acidity is of great interest for alcohol coupling to ethers at low temperature. Rohm and Haas information indicated that the Amberlyst-1010 and Amberlyst-15 resins are stable to 120°C , while the Amberlyst-35 and -36 resins are more thermally stable and can be used to 140°C .

The Amberlyst-1010, -35, and -36 catalysts were subjected to the standard test (p. 26) for screening catalysts for ether synthesis, where the methanol and isobutanol feed rates were both $1.72 \text{ mol.kg cat/hr}$. The temperature was also increased stepwise above 90°C to monitor the temperature dependence of the product formation.

In Tables 10-12, the conversion at 90°C and at some higher temperatures are reported.

Table 10. Amberlyst-1010 Activity as a Function of Temperature

Temperature ($^\circ\text{C}$)	% Methanol Conversion	% Isobutanol Conversion
90	5.0	4.2
100	8.3	8.9
110	14.4	21.3
120	23.6	42.2

Table 11. Amberlyst-35 Activity as a Function of Temperature

Temperature (°C)	% Methanol Conversion	% Isobutanol Conversion
90	16.4	15.8
100	32.1	43.9
110	42.9	63.9
120	62.0	57.1
130	70.0	57.9
90	17.0	15.7

Table 12. Amberlyst-36 Activity as a Function of Temperature

Temperature (°C)	% Methanol Conversion	% Isobutanol Conversion
90	12.3	10.2
100	25.9	30.0
110	42.0	63.1
120	56.7	53.1
130	63.4	57.9
90	10.7	6.8

Amberlyst-1010 showed moderate conversion of both methanol and isobutanol. The Amberlyst-35 and -36 catalysts showed high and similar conversions at all of the reaction temperatures, but Amberlyst-35 tended to be somewhat more active than Amberlyst-36. No deactivation of the Amberlyst-35 catalyst was observed (Table 11). However, in reference to Table 12, some deactivation can be seen for Amberlyst-36, as evidenced upon lowering the reaction temperature back to 90°C after carrying out the reaction at higher temperatures. In comparison with Amberlyst-35 and -36, Amberlyst-15 converted about 10% of methanol and 10% of isobutanol at 90°C. Conversions over all of the polymer resins tested (at 90°C)

during this project are listed in Table 13. The overall order of activity follows the sequence Amberlyst-35 > Amberlyst-36 > Amberlyst-15 \approx Purolite C-150 > BioRad AG 50W X-2 \approx Amberlyst-1010 > Nafion-H.

Table 13. Activity of Polymeric Resin Catalysts at 90°C

Catalyst	% Methanol Conversion	% Isobutanol Conversion
Amberlyst-15	9.1	10.2
BioRad AG 50W X-2	4.9	5.4
Nafion-H	1.4	1.4
Purolite C-150	9.2	9.9
Amberlyst-1010	5.0	4.2
Amberlyst-35	16.4	15.8
Amberlyst-36	12.3	10.2

Selectivity data obtained at the reaction temperatures shown in Tables 10-12 are represented in Figures 6-8. Under the reaction conditions employed, the catalysts were generally rather non-selective, especially at the lower temperatures. At higher temperatures (e.g. $\geq 120^\circ\text{C}$), one product was more dominant than the others. Amberlyst-1010 formed MIBE, DME, and butenes (mainly isobutene) at 90°C , but butenes were favored at temperatures above 90°C . Amberlyst-35 mainly formed butenes at $90-110^\circ\text{C}$, but at 120°C and above DME was predominantly formed (Figure 7). Amberlyst-36 showed a similar selectivity pattern, with butenes being the favored products at 100 and 110°C and DME being the dominant product at 120 and 130°C (Figure 8). Figures 9-14 present the data as % yield of the products. Figures 9-11 give the % yields with respect to the methanol reactant, whereas Figures 12-14 give % yields with respect to isobutanol (fractional conversion times % selectivity). The trends observed in these plots are the same as for the

selectivities in Figures 6-8.

Figure 6. Selectivity for Amberlyst-1010 in mol% of Products.

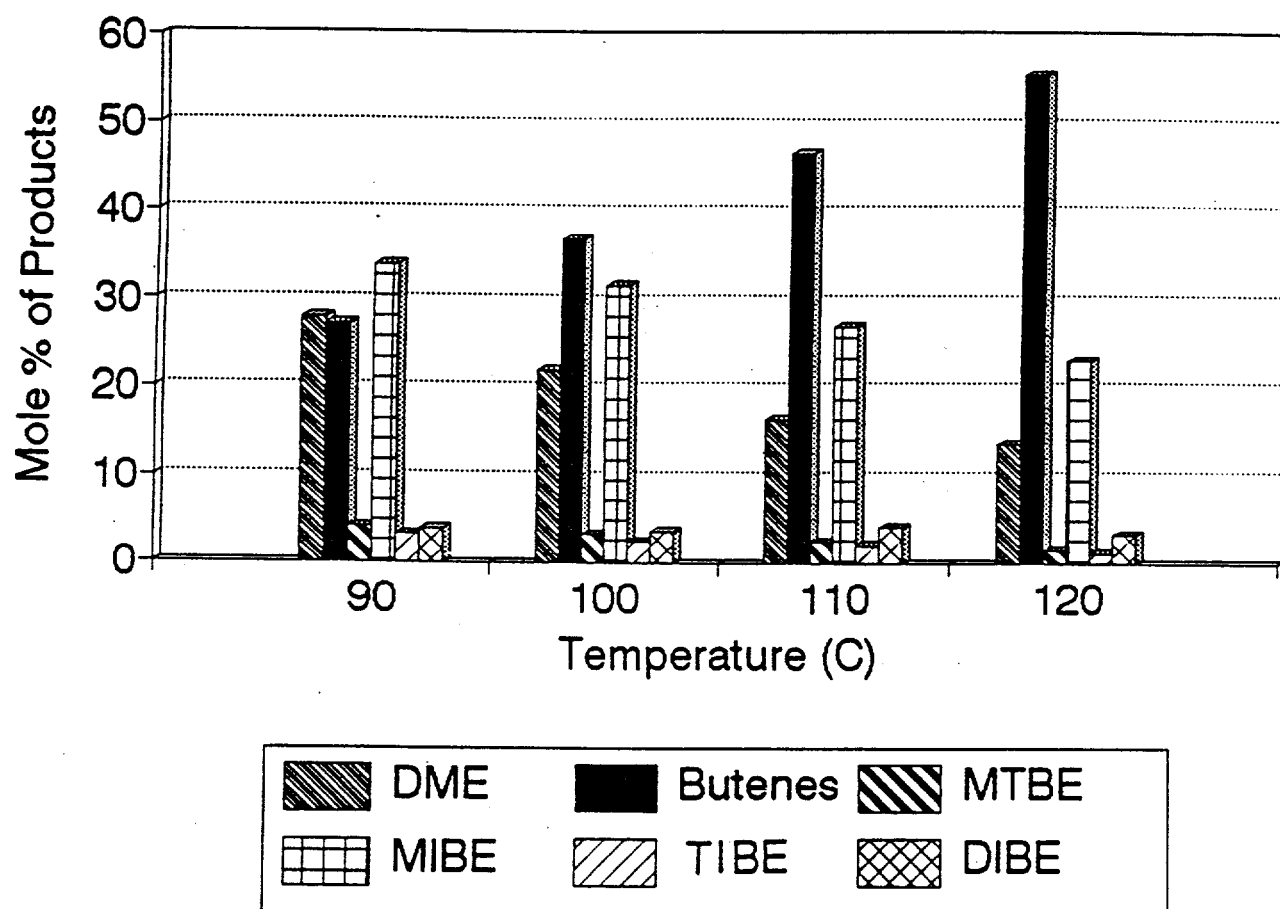


Figure 7. Selectivity for Amberlyst-35 in mol% of Products.

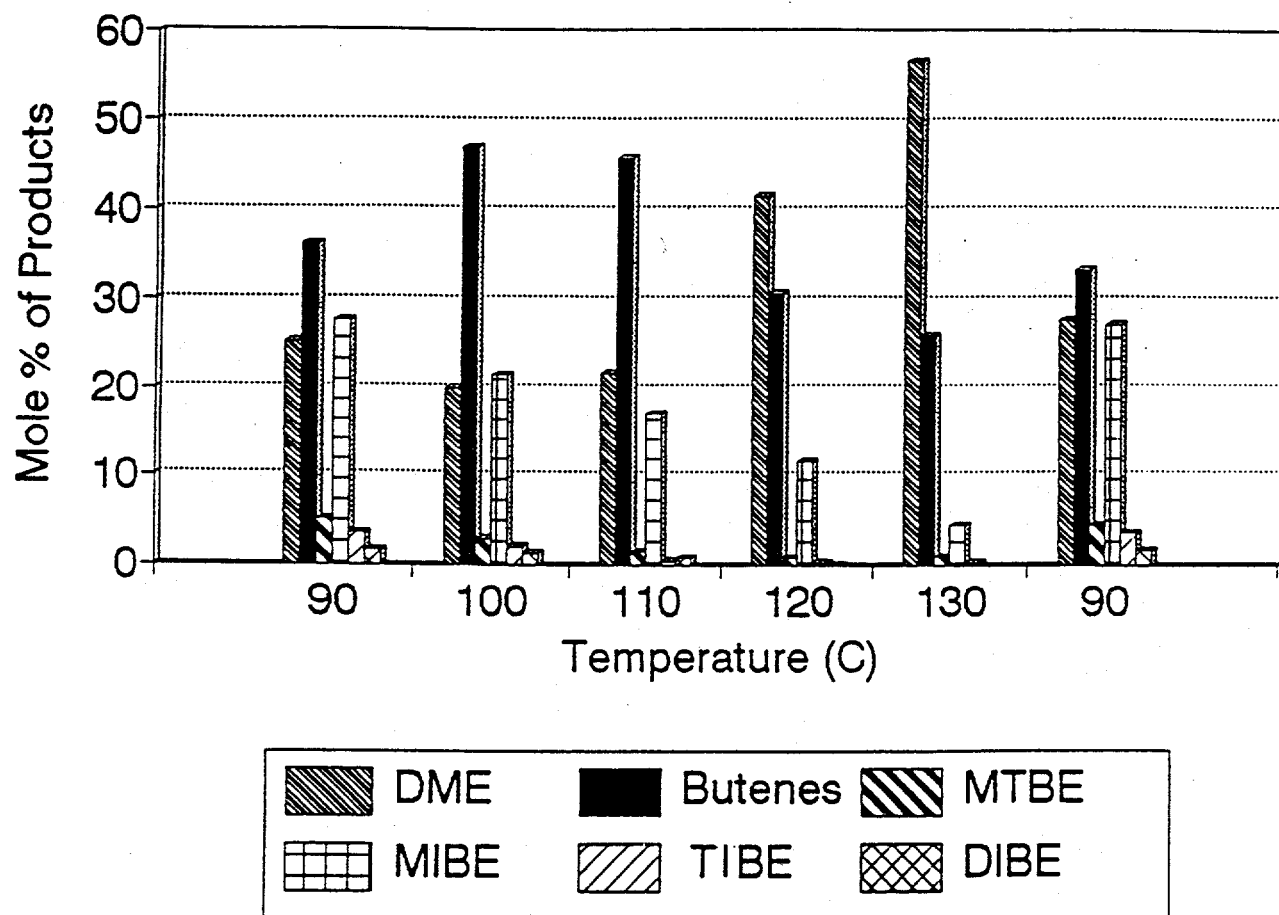


Figure 8. Selectivity for Amberlyst-36 in mol% of Products.

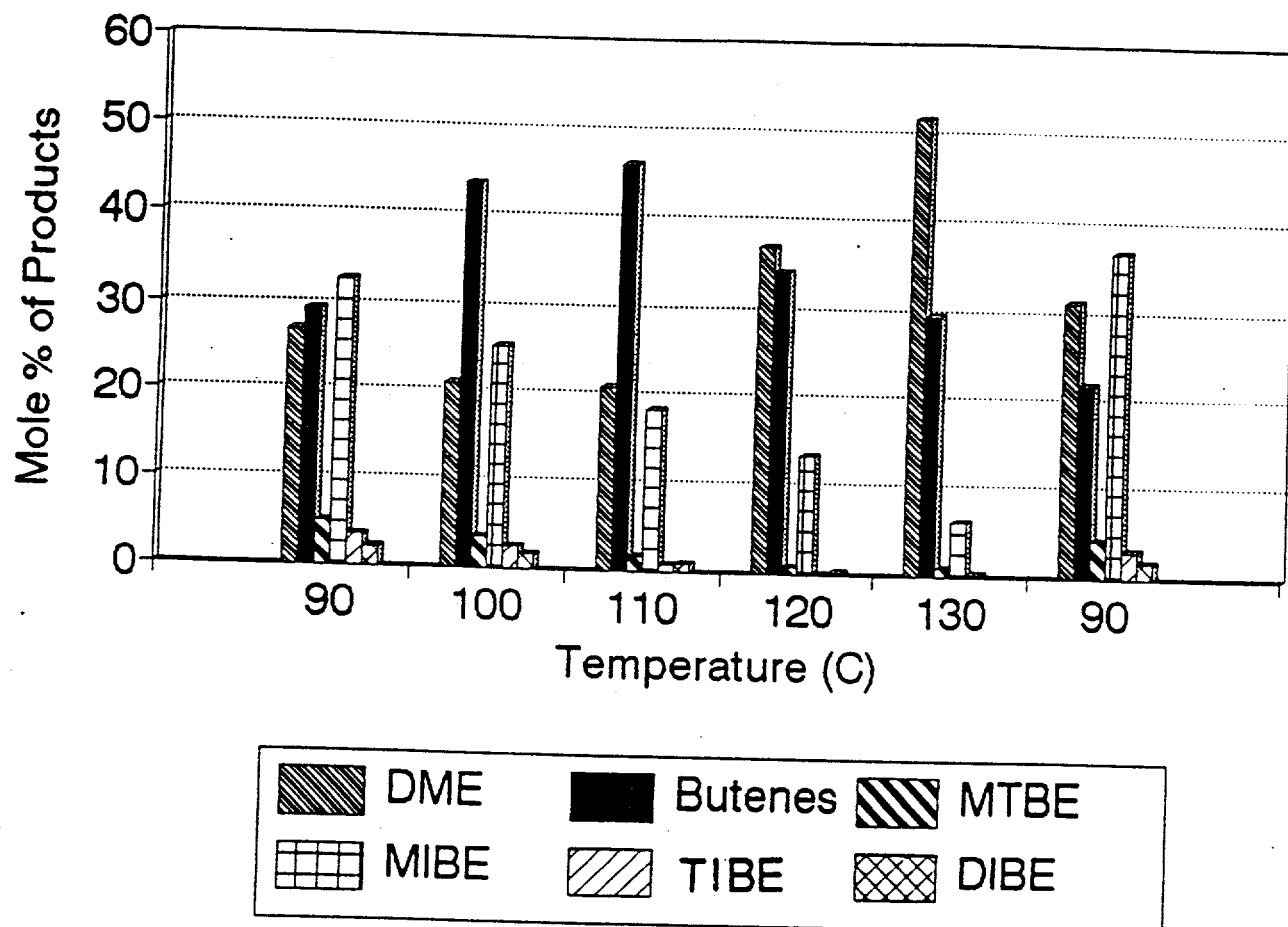


Figure 9. % Yield for Amberlyst-1010 based on Methanol Conversion.

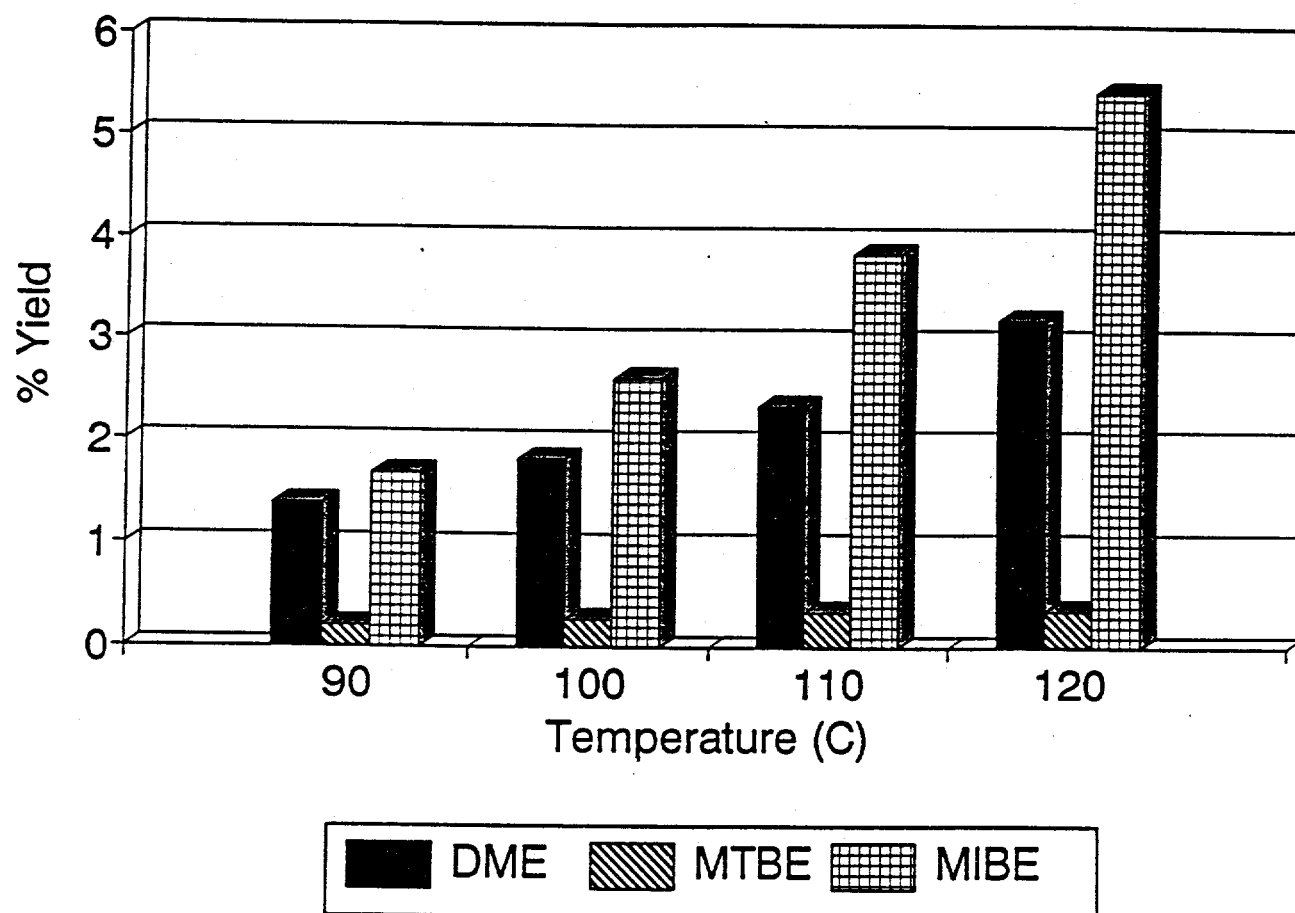


Figure 10. % Yield for Amberlyst-35 based on Methanol Conversion.

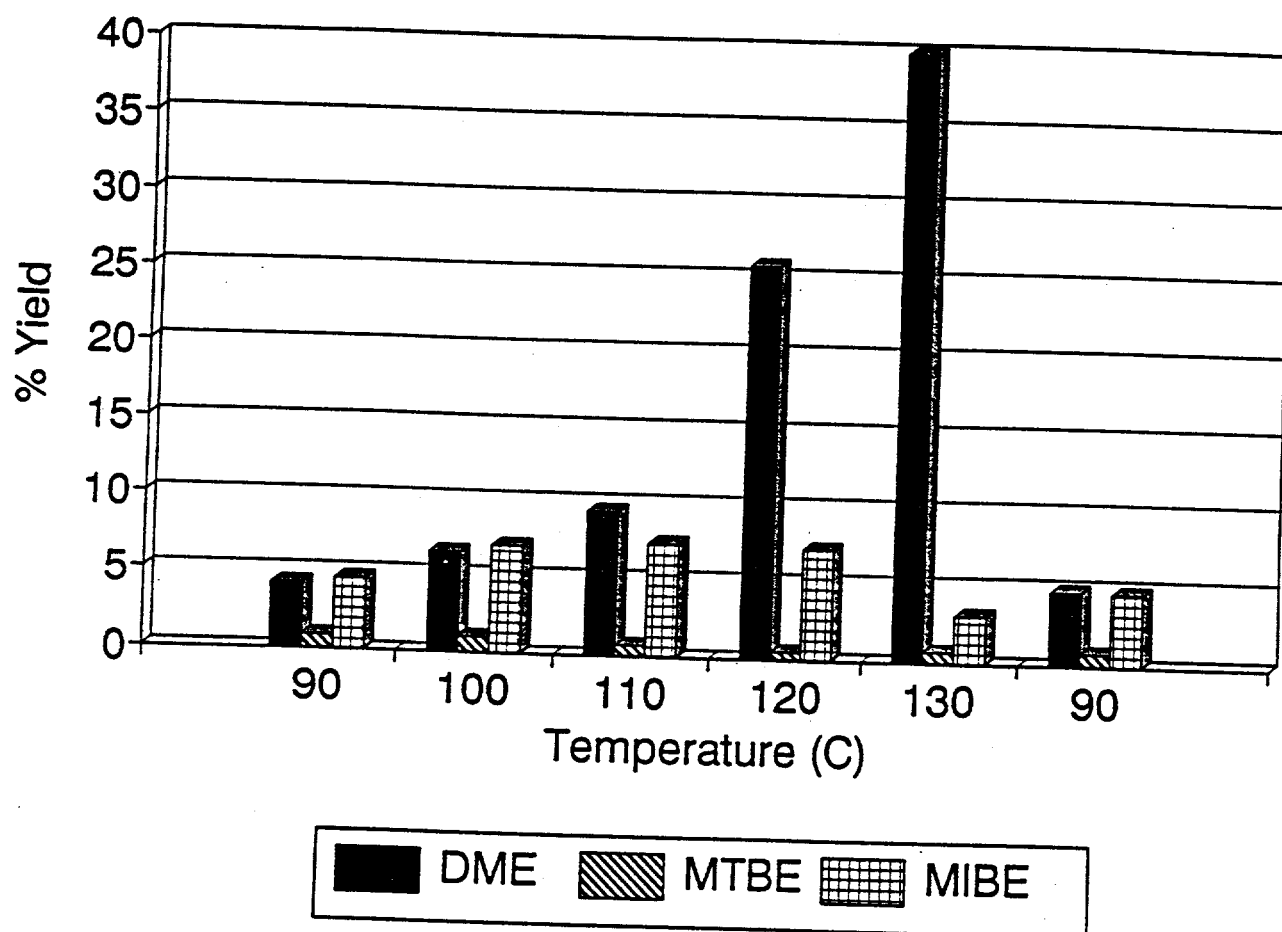


Figure 11. % Yield for Amberlyst-36 based on Methanol Conversion.

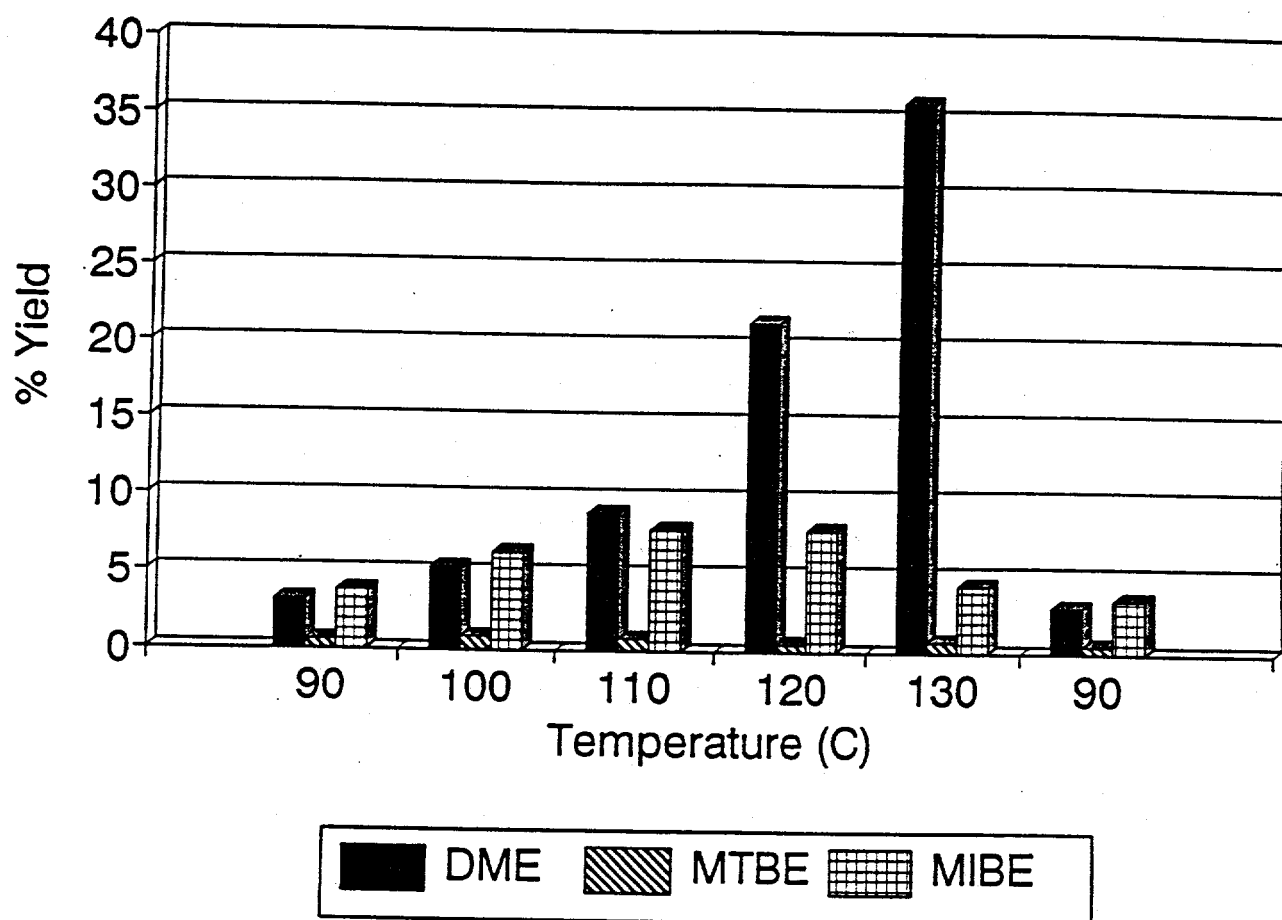


Figure 12. % Yield for Amberlyst-1010 based on Isobutanol Conversion.

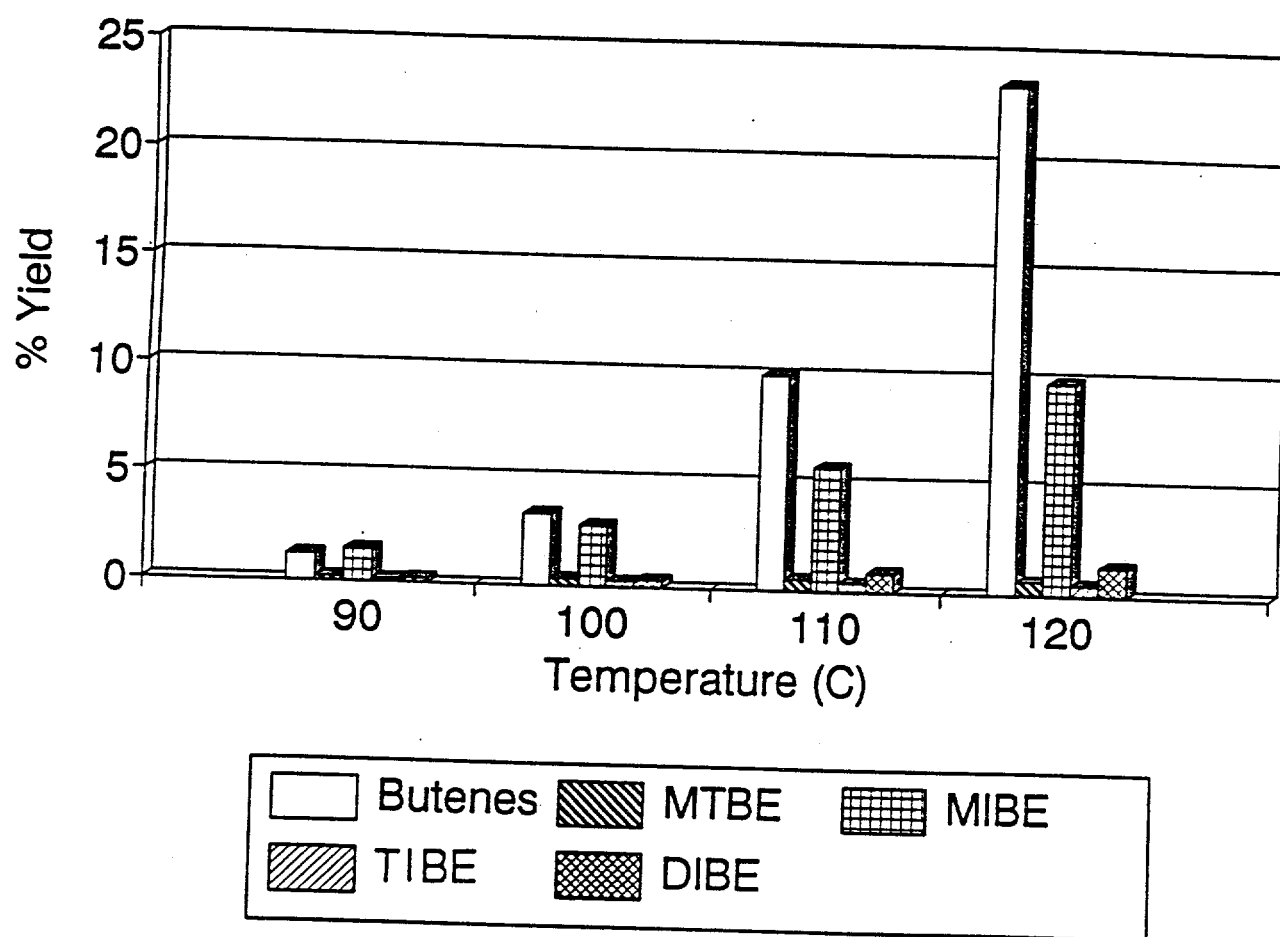


Figure 13. % Yield for Amberlyst-35 based on Isobutanol Conversion.

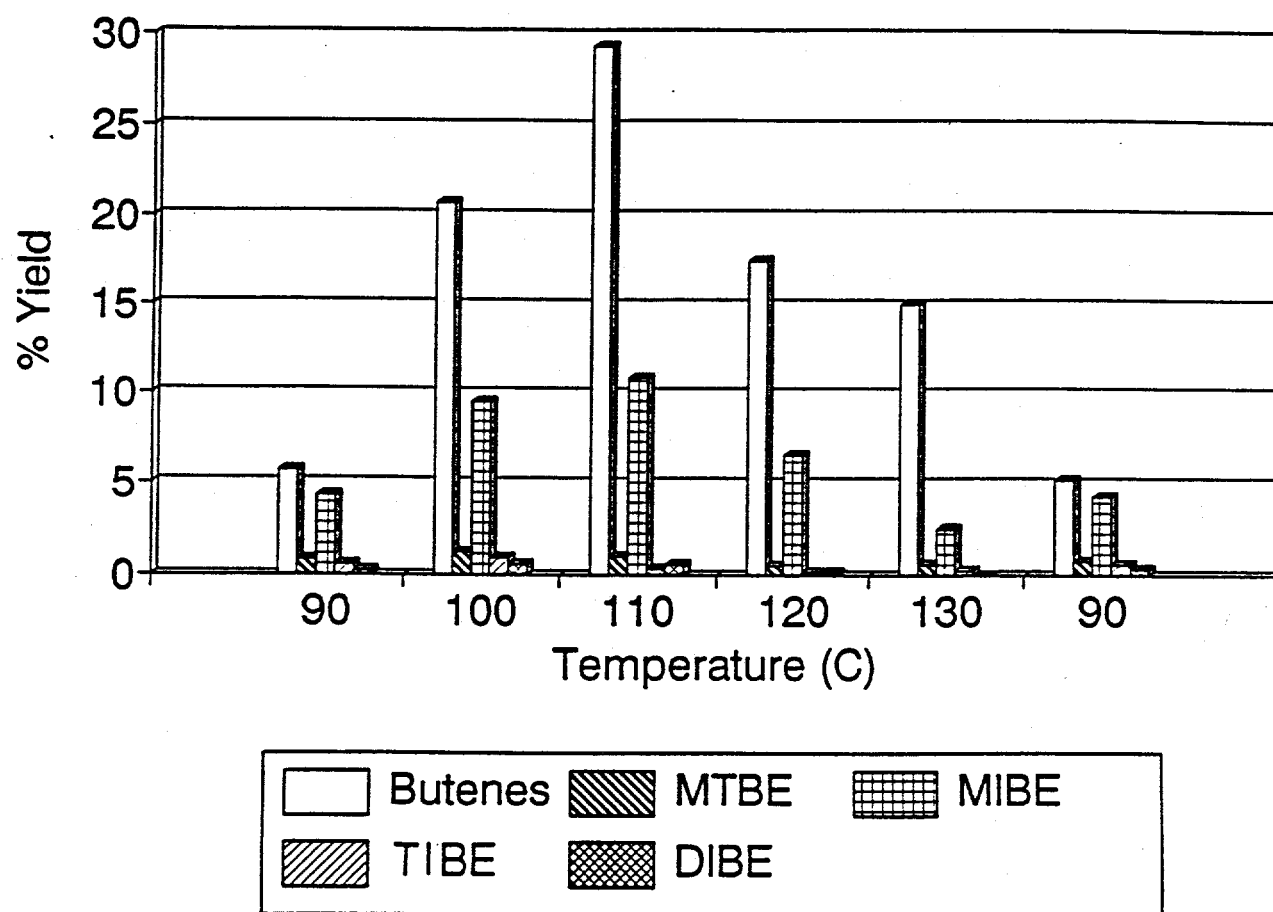
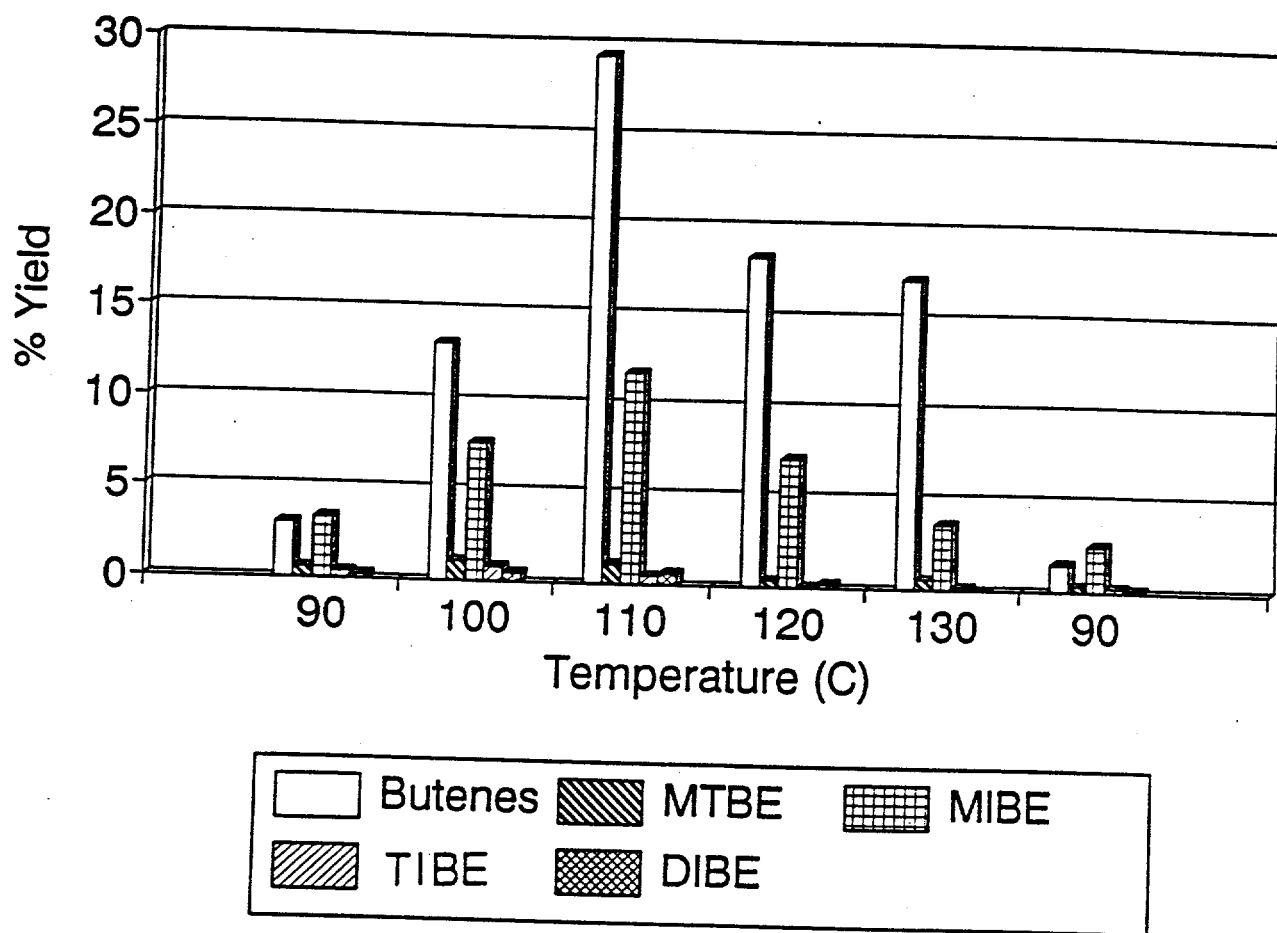


Figure 14. % Yield for Amberlyst-36 based on Isobutanol Conversion.



Pressure Dependence of Amberlyst-35

The reaction of methanol and isobutanol over a Nafion-H catalyst had previously been shown to be very sensitive to the total pressure (16,17). To investigate the pressure dependence of the synthesis reaction over Amberlyst-type catalysts, the active Amberlyst-35 resin was chosen. The pressure dependence study was carried out at the two reaction temperatures of 90 and 117°C.

The experiment was carried out using the following conditions:

Catalyst weight	1.0 g dry catalyst
Temperature	90 and 117°C
Total pressure at 90°C	0.1-0.65 MPa
Total pressure at 117°C	0.1-1.3 MPa
Methanol feed	10.4 mol/kg cat/hr
Isobutanol feed	5.2 mol/kg cat/hr
He + N ₂	185 mol/kg cat/hr

This includes the standard temperature of 90°C and pressure of 0.1 MPa developed for testing the resin catalysts.

The results shown in Figures 15 and 16 demonstrate that the formation of butenes was very sensitive to the alcohol partial pressure. A small elevation of the alcohol pressure suppressed the formation of butenes rather drastically at both 90 and 117°C. The synthesis rates of DME, MIBE, and MTBE were not strongly affected by pressure at 90°C, although there was a trend to increase the space time yield of DME as the alcohol pressure was increased. At the reaction temperature of 117°C, all of the ethers showed increasing productivities as the pressure of the reactants was increased (Figure 16).

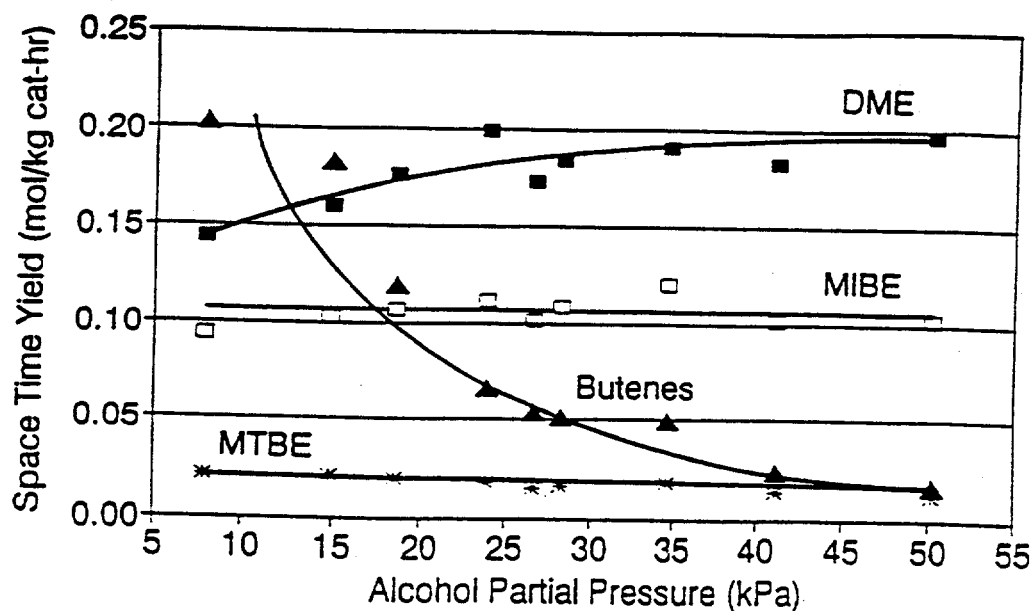


Figure 15. Space Time Yields of the Ethers and Butenes Formed Over Amberlyst-35 as a Function of the Alcohol Partial Pressure at 90°C.

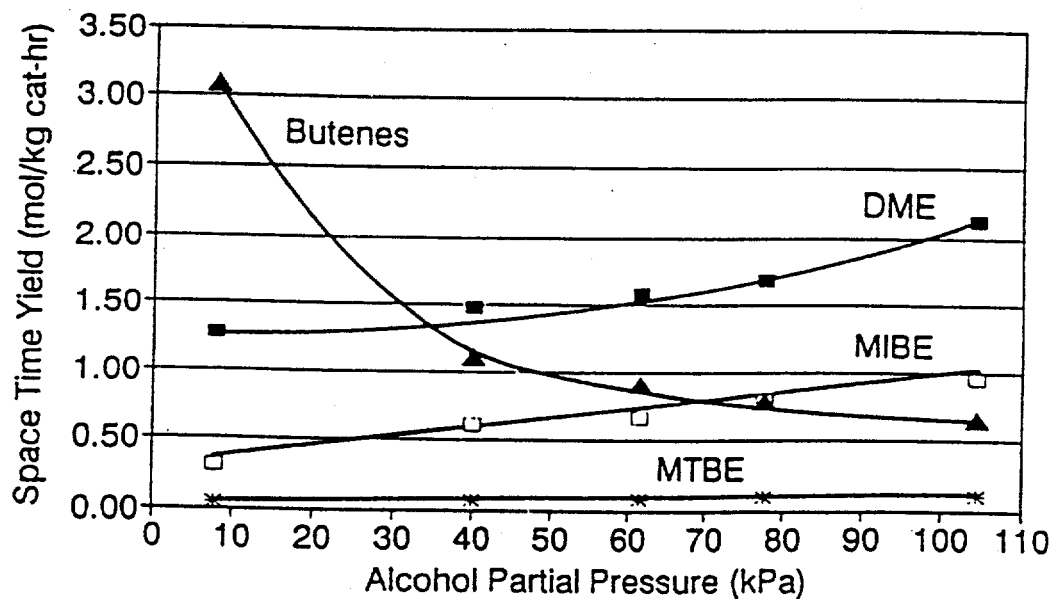


Figure 16. Space Time Yields of the Ethers and Butenes Formed Over Amberlyst-35 as a Function of the Alcohol Partial Pressure at 117°C.

E. Mechanism of MIBE Formation Over Nafion-H: Isotope Labelling Study of Ether Synthesis Over Nafion-H

The two reactant alcohols, methanol and isobutanol, can be produced from H_2/CO synthesis gas (a non-petroleum feedstock) over alkali-promoted Cu/ZnO catalysts (13,14,24). Since MTBE is an oxygenated, high octane fuel additive and MIBE has a high cetane number of 53 (25), it is desirable to shift the selectivity of the alcohol coupling reaction to control MIBE or MTBE as required by fuel composition. It has been shown that in the reaction of methanol with isobutanol, MTBE is the thermodynamically favored oxygenated product but that MIBE is the kinetically favored product (17). Therefore, an isotope labelling experiment was carried out to provide mechanistic insight into the manner in which methanol and isobutanol react together to form DME, MIBE, and MTBE and to determine if MTBE were derived from MIBE.

The methanol was purchased from MSD Isotopes and was 97.3 atom% ^{18}O enriched. Anhydrous isobutanol was purchased from Aldrich Chemical Co., Inc., and it contained the natural abundances of oxygen isotopes, i.e. 99.8% ^{16}O and 0.2% ^{18}O . Nafion-H microsaddles was the catalyst employed in this study. The alcohols were mixed in a molar ratio of 1/1 and pumped into the preheater section of the reactor at the rate of 3.4 mol/kg catalyst/hr by means of a Gilson high pressure pump. The reaction took place in a gas phase tubular downflow reactor with on-line GC analysis. Conversions of methanol and isobutanol were kept below 10% to minimize any possible secondary reactions and to keep the reaction within the differential regime. Isotopic composition analysis was accomplished off-line *via* GC/MS analysis, following the trapping and condensation of the effluent from the reactor in a dry ice cooled cold-finger. The mass spectra were compared to those of reference compounds for identification of the catalytic products (26).

The experimental testing conditions that were utilized consisted of the following:

Catalyst weight	2.00 g (dry)
Reaction temperature	90°C
Total Pressure	0.1 MPa
Molar ratio MeOH/iBuOH	1/1
Methanol flow rate	1.7 mol/kg cat/hr
Isobutanol flow rate	1.7 mol/kg cat/hr
He + N ₂ flow rate	16.6 mol/kg cat/hr

The molar abundances of each ¹⁶O- or ¹⁸O-containing product were quantified *Via* GC/MS analyses by comparing the most intense MS peak intensities to one another. It was observed that the most abundant fragment from both DME and MIBE (easily separated by GC) was CH₃OCH₂ (after the loss of the CH(CH₃)₂ part of the MIBE molecule, which was further fragmented), while from MTBE it was (CH₃)₃CO (after the loss of the CH₃ group). Specifically, for MIBE analysis, the peak at a mass-to-charge (m/q) ratio = 47 was normalized to the most intense peak at m/q = 45, corresponding to the CH₃-¹⁶O-CH₂ fragment (26), in order to calculate the fraction of ¹⁸O-containing MIBE relative to ¹⁶O-containing MIBE, respectively. Likewise for MTBE, the peaks at m/q = 75 and 73 (26), corresponding to the (CH₃)₃-C-¹⁸O and (CH₃)₃-C-¹⁶O fragments, respectively, were used, while the m/q = 47 peak intensity, corresponding to the CH₃-¹⁸O-CH₂ fragment, was compared to that of the m/q = 45 peak (CH₃-¹⁶O-CH₂) for DME quantification. Other less intense MS peaks were also analyzed for further verification of the analyses.

The space time yields of the products are given in Table 14, and it is seen that MIBE was the principal product, while similar but smaller quantities of DME and isobutene were also formed. Analyzable quantities of MTBE were also formed.

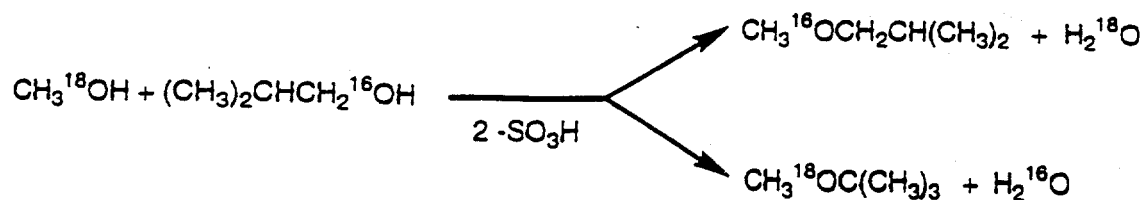
Table 14

Space Time Yields of Products Formed by the Reaction of ^{18}O -Methanol and ^{16}O -Isobutanol over Nafion-H at 90°C and 101 kPa.

Product	Space-Time-Yields ($\text{mol (kg catalyst)}^{-1} \text{ hr}^{-1}$)
MIBE	0.0140
DME	0.0045
Isobutene	0.0037
MTBE	0.0010
C_8 -Ethers	trace

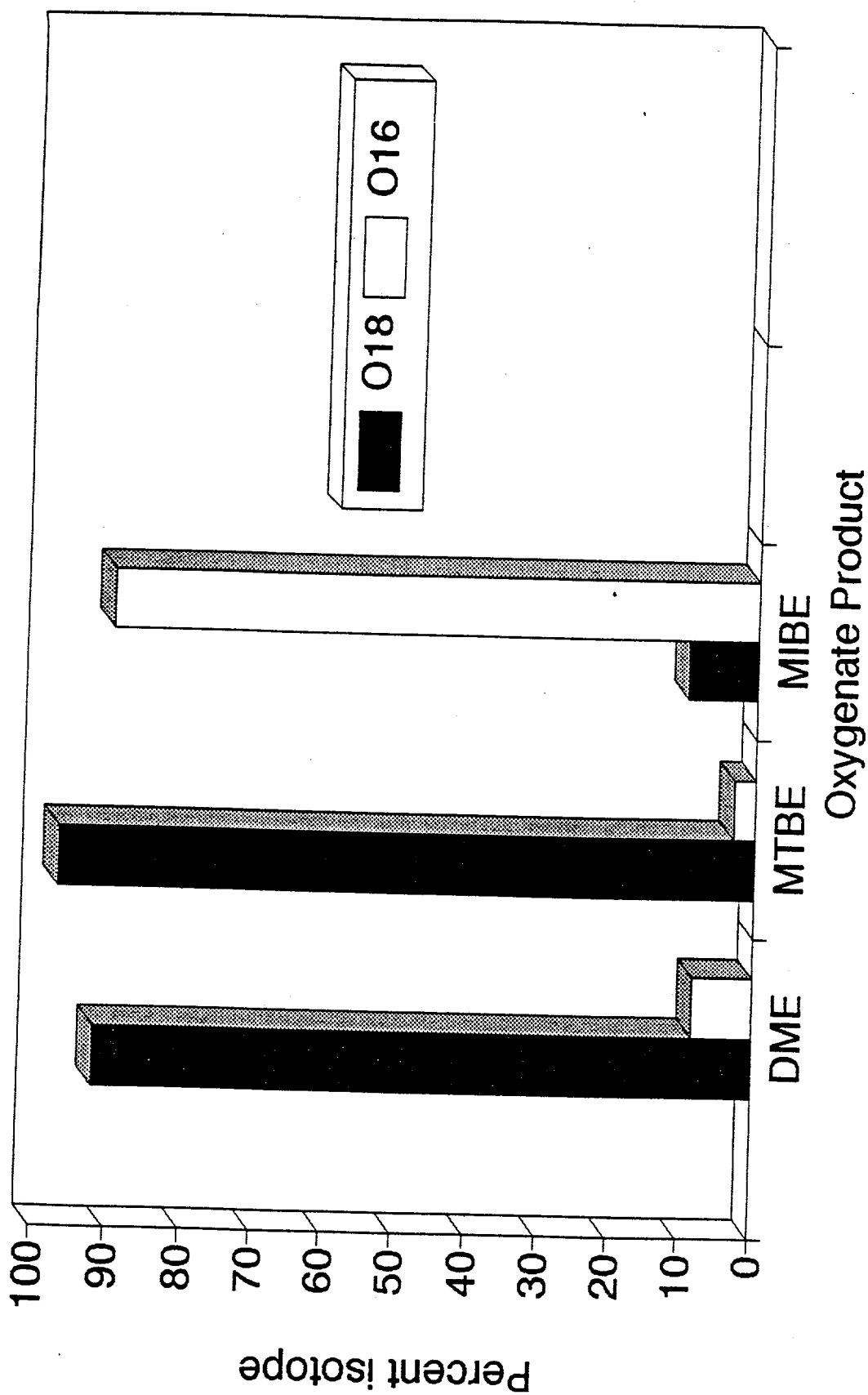
Isotopic composition of each of the oxygenates formed was determined by mass spectrometry as described. The results of these analyses are presented in Figure 17. The oxygen-containing products ^{16}O -MIBE and ^{18}O -MTBE were found with over 90% selectivity. The isotopic composition of DME of $\approx 92\%$ ^{18}O demonstrates that isotopic scrambling of methanol did not occur to a significant extent over the catalyst.

These results can be summarized as follows:



It is evident from these results that MIBE derived its oxygen from isobutanol, while MTBE obtained its oxygen from methanol. This result demonstrates that MIBE and MTBE are not formed from a common intermediate and that MTBE is not the product of isomerization of MIBE. Moreover, MIBE is produced by a kinetically controlled pathway

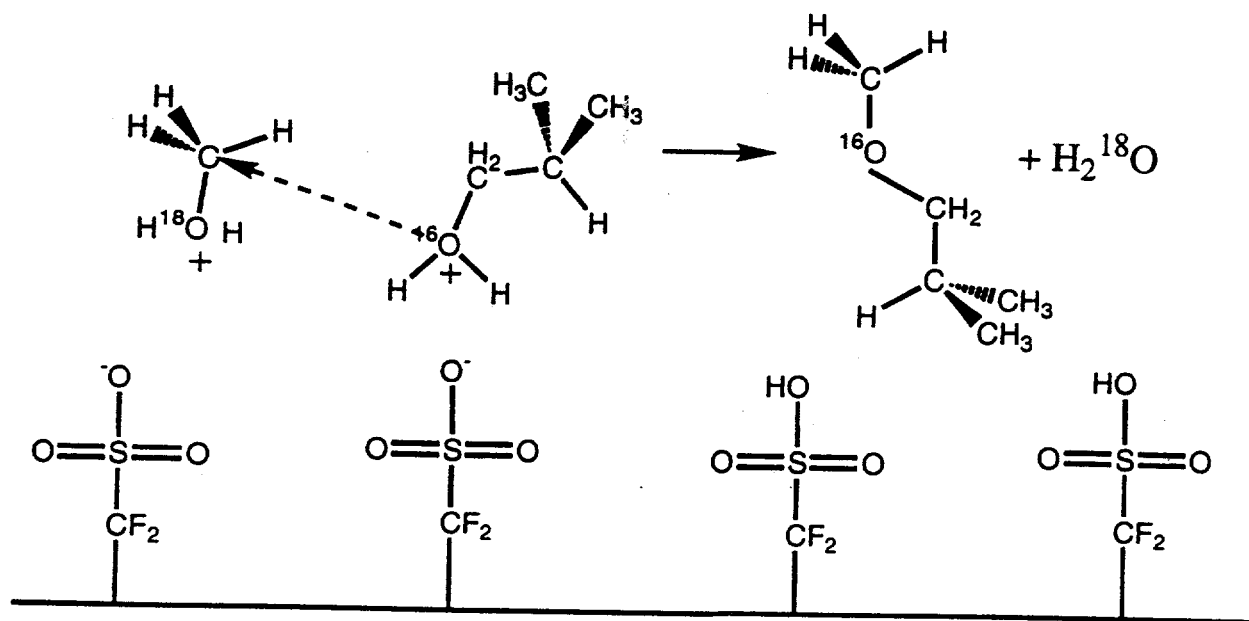
Figure 17. Isotopic composition of the reaction of ^{18}O -methanol and ^{16}O -isobutanol over the Nafion-H catalyst at 90°C .



that is mechanistically more efficient than that leading to the thermodynamically more stable MTBE. These isotope discriminating reactions, taken in conjunction with those of the prior kinetic analyses (17), support a reaction scheme for MIBE that has mechanistic features of a S_N2 solution-phase reaction, but the heterogeneous synthesis exhibits distinctly different kinetics unique to surface catalyzed reactions in which both alcohols are activated by being adsorbed on the acid sites of the Nafion-H catalysts. This results in kinetics that show self-poisoning of the reaction by either alcohol at its high concentration, contrary to the kinetics of S_N2 reactions in solutions in which the rate is proportional to the concentrations of both reactants (27). In fact, the surface-catalyzed four-center reaction (involving two SO_3H surface groups and the two alcohols) exhibits a maximum rate at optimum concentrations of the reactant alcohols, which falls off when either alcohol is in excess as a negative power of the partial pressure of the excess reactant (17).

The specific mode of bonding of the alcohols to the sulfonic acid sites has not been resolved in full detail, but the current ^{18}O label flow to the products rules out the formation of isobutyl ester or isobutyl carbenium ion put forward as a possibility earlier (17), as in this case isobutanol would lose its oxygen and MIBE would gain ^{18}O from methanol, contrary to experiment. A likely type of bonding is *via* oxonium of the alcohols, with methanol oxonium suffering a rear attack by isobutanol that is just leaving its bonded state on neighboring sulfonic group; the ^{18}O -labelled H_2O is then the leaving group from methanol and the MIBE produced retains ^{16}O from isobutanol, as shown in Figure 18. The reverse attack of isobutyl oxonium by methanol is sterically hindered, in analogy with steric hindrance of the attack of isobutyl group by ethoxide in the related S_N2 reactions of alkyl halides (27).

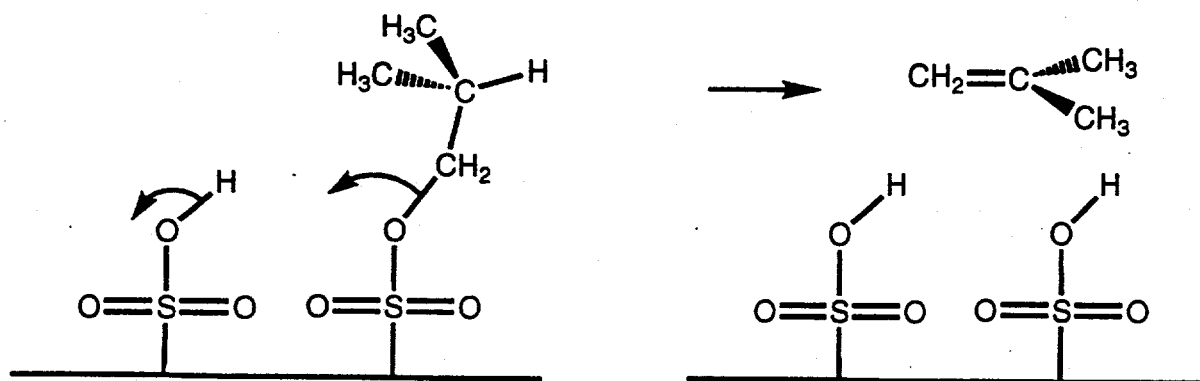
Figure 18. The Reaction Pathway for ^{18}O -Methanol and ^{16}O -Isobutanol to Form ^{16}O -MIBE.



Contrary to MIBE, the MTBE contained almost exclusively oxygen originating from methanol and not isobutanol. Since isobutanol is dehydrated to isobutene by a parallel reaction, the origin of MTBE can be traced to a coupling of isobutene with methyl oxonium or isobutyl carbenium with methanol (28), as shown in Figure 19. The former path has been proposed to occur in the industrial acid-catalyzed MTBE synthesis from methanol and isobutene (29).

Figure 19. The Mechanism for Isobutanol Dehydration to Form Isobutene, with Subsequent Reaction of O^{18} -Methanol to Form O^{18} -MTBE.

Mechanism for i-BuOH dehydration to i-butene



Subsequent reaction of $Me^{18}OH$ with i-butene to MTBE

